

SCIENTIFIC REPORTS

OPEN

MtrA of the sodium ion pumping methyltransferase binds cobalamin in a unique mode

Tristan Wagner¹, Ulrich Ermler² & Seigo Shima^{1,3}

Received: 04 January 2016

Accepted: 01 June 2016

Published: 21 June 2016

In the three domains of life, vitamin B₁₂ (cobalamin) is primarily used in methyltransferase and isomerase reactions. The methyltransferase complex MtrA–H of methanogenic archaea has a key function in energy conservation by catalysing the methyl transfer from methyl-tetrahydromethanopterin to coenzyme M and its coupling with sodium-ion translocation. The cobalamin-binding subunit MtrA is not homologous to any known B₁₂-binding proteins and is proposed as the motor of the sodium-ion pump. Here, we present crystal structures of the soluble domain of the membrane-associated MtrA from *Methanocaldococcus jannaschii* and the cytoplasmic MtrA homologue/cobalamin complex from *Methanothermobacter fervidus*. The MtrA fold corresponds to the Rossmann-type α/β fold, which is also found in many cobalamin-containing proteins. Surprisingly, the cobalamin-binding site of MtrA differed greatly from all the other cobalamin-binding sites. Nevertheless, the hydrogen-bond linkage at the lower axial-ligand site of cobalt was equivalently constructed to that found in other methyltransferases and mutases. A distinct polypeptide segment fixed through the hydrogen-bond linkage in the relaxed Co(III) state might be involved in propagating the energy released upon corrinoid demethylation to the sodium-translocation site by a conformational change.

In the methanogenic pathway from H₂ and CO₂, the membrane-spanning methyl-tetrahydromethanopterin (CH₃-H₄MPT):coenzyme M (CoM-SH) methyltransferase complex (MtrA–H) catalyses the exergonic methyl transfer from CH₃-H₄MPT to CoM-SH ($\Delta G^{o'} = -30$ kJ/mol) coupled with endergonic sodium-ion gradient formation¹. In methanogens lacking cytochromes, the MtrA–H reaction represents the only chemiosmotic process^{1–3}. The generated electrochemical membrane potential is used for ATP biosynthesis from ADP and inorganic phosphate by A₁A₀ ATP synthase⁴.

The molecular organization of the MtrA–H complex and its catalysed reactions are outlined in Fig. 1 (see also Supplementary Figure S1). Primary structure analysis predicts MtrC, MtrD and MtrE as integral membrane proteins with at least six transmembrane helices, MtrA, MtrB, MtrF and MtrG as peripheral proteins with one transmembrane helix anchor, and MtrH as a peripheral protein without a membrane anchor^{1,5,6}. The only prosthetic group required for catalysis is vitamin B₁₂ (cobalamin) bound to MtrA. According to a previous electron paramagnetic resonance (EPR) spectroscopy and site-directed mutagenesis analyses^{7–11}, cobalt of the corrinoid in the inactive Co(II) state is axially coordinated by a histidine (His84 of MtrA from *Methanothermobacter marburgensis*) imidazolium group (base-off/His-on configuration) rather than by the dimethylbenzimidazole base as a fifth ligand^{9–11}.

The MtrA–H reaction starts with a methyl group transfer from methyl-H₄MPT bound to MtrH to the upper ligation site of cob(I)alamin ($\Delta G^{o'} =$ approximately -15 kJ/mol)^{1,6}. Subsequently, the methyl group of the generated methyl-cob(III)alamin is transferred to CoM-SH in the presence of sodium ions ($\Delta G^{o'} =$ approximately -15 kJ/mol)^{1,8}. This finding points towards the participation of the demethylation reaction in sodium-ion translocation¹², which is probably localized on MtrE as it contains a characteristic aspartate in the transmembrane helix^{1,5}. Based on the intensively studied coordination and redox chemistry of cobalamins, the histidine ligand is not coordinated to cobalt in the reduced non-methylated cob(I)alamin form (base-off/His-off), which is in contrast to the methylated cob(III)alamin form (base-off/His-on)^{1,8,13}. Therefore, it has been proposed that the dissociation of the His ligand during formation of cob(I)alamin from methyl-cob(III)alamin induces conformational

¹Max Planck Institute for Terrestrial Microbiology, Karl-von-Frisch-Straße 10, 35043 Marburg, Germany. ²Max Planck Institute of Biophysics, Max-von-Laue-Straße 3, 60438 Frankfurt am Main, Germany. ³PRESTO, Japan Science and Technology Agency (JST), 4-1-8 Honcho Kawaguchi, 332-0012 Saitama, Japan. Correspondence and requests for materials should be addressed to S.S. (email: shima@mpi-marburg.mpg.de)

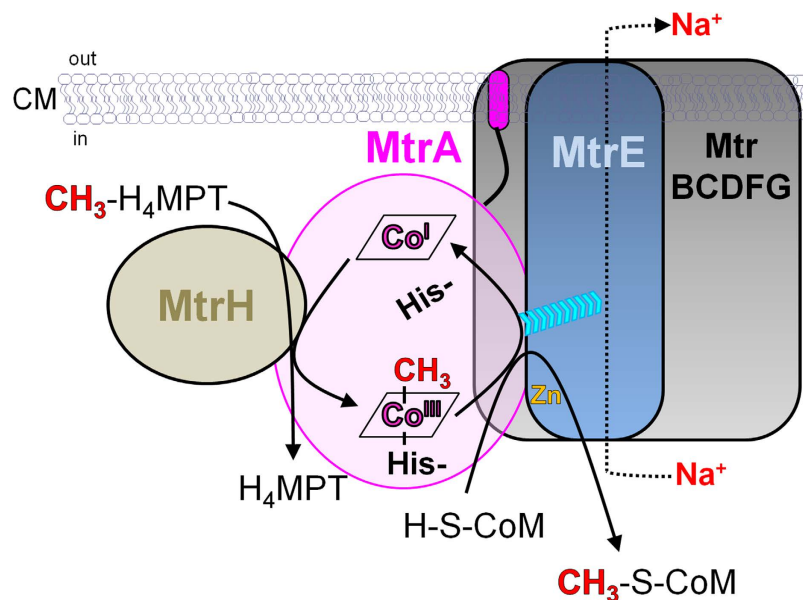


Figure 1. Organization and catalytic cycle of the MtrA–H complex. In a two-step reaction, the methyl group of methyl-tetrahydromethanopterin ($\text{CH}_3\text{-H}_4\text{MPT}$) bound to MtrH is first transferred to cobalamin bound to MtrA and second from there to coenzyme M (CoM-SH). It is postulated that the latter methyl-transfer reaction provokes sodium-ion translocation localized on MtrE¹. The cyan arrowheads indicate energy transfer from the displaced histidine to MtrE upon its dissociation from Co(I). The sketched size of the subunits does not correspond to their molecular masses. CM: cytoplasmic membrane.

rearrangements of parts of MtrA¹. From there, the energy is transmitted to MtrE, thereby causing sodium ion translocation (Fig. 1 and Supplementary Fig. S2)¹².

Enzymes carrying a prosthetic group derived from vitamin B₁₂ (referred to as B₁₂ enzymes) can be grouped into those containing a Rossmann fold-like open α/β domain^{14,15} (termed Rossmann-type domain) such as methionine synthase¹⁶, methanol cobalamin methyltransferases¹⁷, iron-sulphur corrinoid methyltransferases^{18,19}, methyl-malonyl-CoA mutases²⁰ and glutamate mutases²¹, and those with other folds, such as reductive dehalogenases²² and glycerol and diol dehydratases^{23,24}. Vitamin B₁₂-dependent trafficking and membrane transport proteins were not taken into account. Methyltransferases and mutases contain the consensus sequence DXHXXG-41–42-SXL-26–28-GG for binding cobalamin^{1,16,17,25}; although iron-sulphur cobalamin methyltransferases are the exception^{18,19}. MtrA has no overall sequence similarity to any B₁₂ enzyme and lacks the common fingerprint motif.

Genome analysis has revealed an extra copy or copies of the *mtrA* gene in many methanogenic archaea (e.g., *M. marburgensis*, *Methanobacterium formicum*, *Methanobrevibacter ruminantium*, *Methanothermobacter fervidus* and *Methanosarcina barkeri*). These cytoplasmic MtrA homologues consist only of a soluble cobalamin-binding domain of 170–180 amino acids, which is in contrast to the approximately 250 amino acids of membrane-associated MtrA. Truncated MtrA and MtrA homologues of methanogens have a sequence identity of 60–97%. MtrA homologues have also been identified in the genomes of some bacteria and non-methanogenic archaea. Despite their low sequence identity compared to membrane-associated MtrA (~40%), the key residue His84 is mostly conserved.

Membrane-associated MtrA devoid of the C-terminal transmembrane helix was over-produced in *Escherichia coli* 20 years ago in a soluble but cobalamin-free form, and the holoenzyme was reconstituted by unfolding and refolding in the presence of cobalamin¹¹. However, cobalamin appears to bind less tightly to isolated MtrA than to MtrA in the MtrA–H complex. Here, we report on the X-ray structures of the B₁₂-binding domain of membrane-associated MtrA from *Methanocaldococcus jannaschii* and of the MtrA homologue from *M. fervidus* in complex with cobalamin. Analyses of these structures reveal a cobalamin-binding site that differs from other B₁₂-binding proteins in an unexpected manner and also provides initial hints of how the energy of cobalt demethylation is transformed into conformational energy used for the ultimate sodium-ion translocation process.

Results and discussion

Experimental basis. To structurally characterize cobalamin-binding MtrA, we overproduce the soluble domain of MtrA of *M. jannaschii*, *M. marburgensis*, *M. evestigatum* and *M. kandleri* and the cytoplasmic MtrA homologues from *M. fervidus* and *M. evestigatum*. The use of the cytoplasmic MtrA homologues as models for MtrA in order to increase the crystallization space is justified because of the high sequence identity, e.g. 97% between membrane-associated MtrA and the MtrA homologue of *M. fervidus*. Because of the stability of bound B₁₂, we used the MtrA homologue of *M. fervidus* and the genetically truncated MtrA of *M. jannaschii* (see Materials and methods).

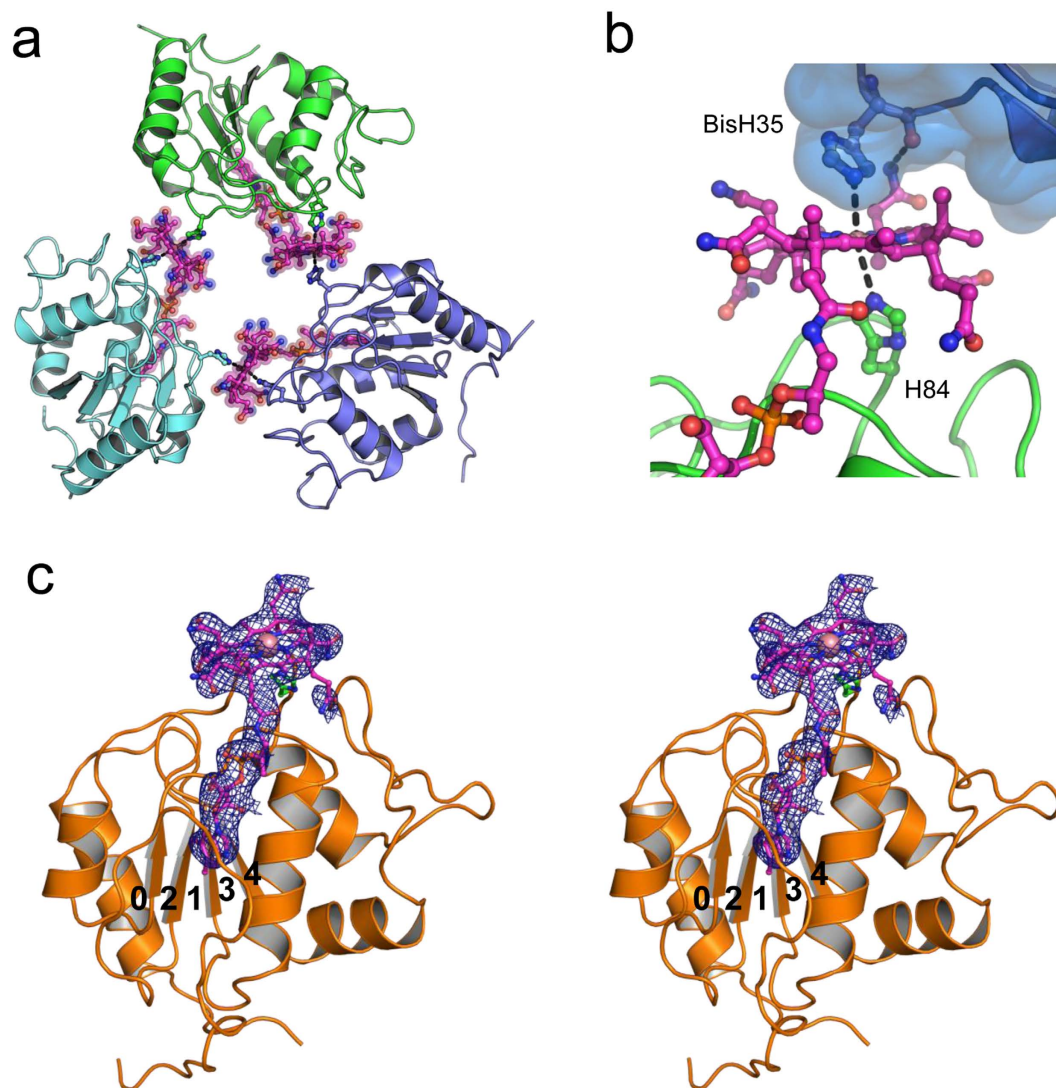


Figure 2. Structure of the cytoplasmic MtrA homologue from *M. fervidus*. (a) Triangular arrangement of the three MtrA homologues (green, blue, cyan) in the asymmetric unit. Cobalamin, the lower axial ligand (His84) and the artificial sixth axial ligand (His35 from the neighbouring MtrA) are shown as ball and stick models (carbons for B₁₂ in pink). (b) The bisHis ligation structure of the cobalt is shown in detail. A significant contact area between the subunits is absent. (c) Rossmann-type fold of the MtrA homologue. The 2F_o-F_c map at the cobalamin molecule is contoured at 1.0 σ (blue mesh).

The cytoplasmic MtrA homologue from *M. fervidus* was produced by heterologous expression as the cobalamin-free apoenzyme. The holoenzyme was subsequently reconstituted after unfolding and refolding by dilution with a buffer containing either methylcobalamin or hydroxocobalamin. Both refolded MtrA solutions were pink and showed characteristic UV/Vis spectra of cob(III)alamin (Supplementary Fig. S3). After 1 day of incubation, the reconstituted MtrA homologue–hydroxocobalamin complex solution turned orange; the UV-Vis spectrum revealed the cob(II)alamin state (Supplementary Fig. S3)²⁶. The tight binding of cobalamin to the MtrA homologue was verified by gel filtration and SDS-PAGE of unheated samples (Supplementary Fig. S4)¹¹. Crystals of the MtrA homologue containing hydroxocobalamin grew after one year, and a unique crystal diffracted to 3.0 Å resolution. Phases were determined by using the single-wavelength anomalous dispersion method with cobalt as the anomalous scatterer. The structure revealed three cytoplasmic MtrA molecules in an asymmetric unit arranged as a homotrimer with a three-fold symmetry (Fig. 2). The trimer was mainly linked together by a covalent bond between the cobalt of cobalamin of one molecule and His35 of its neighbour. Cytoplasmic MtrA in complex with methyl-cobalamin did not crystallize under these conditions; the methyl group bound to cobalamin may prevent the coordination between cobalt and His35 of the neighbouring molecule. The occupancy of the upper axial ligation site by a histidine is presumably not physiologically relevant because the enzyme needs to switch from Co(I) to CH₃-Co(III) during the reaction¹. The absence of a significant contact area between the subunits is in line with this assumption (Fig. 2b).

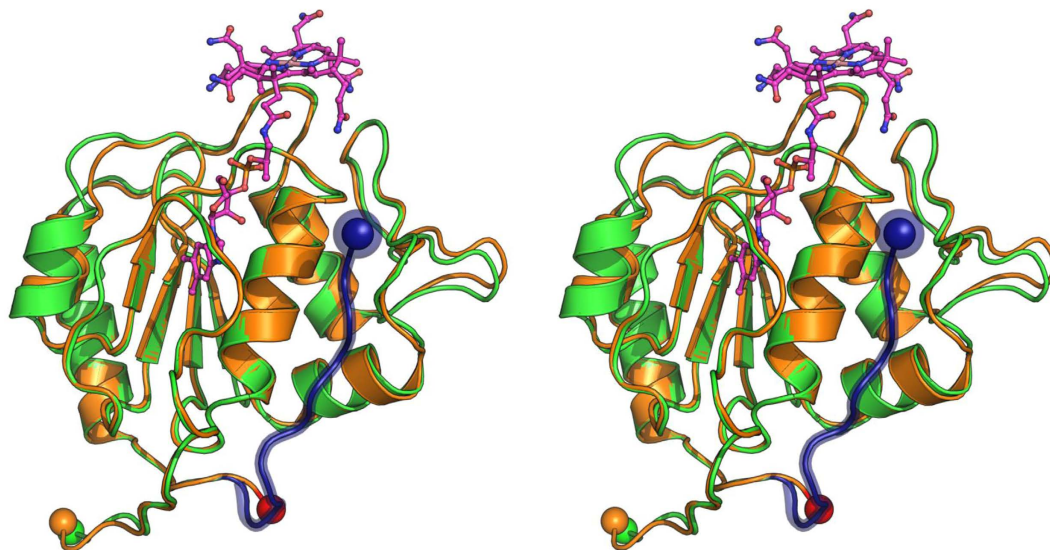


Figure 3. Structure of the soluble domain of the membrane-associated MtrA from *M. jannaschii*.

The soluble domain of membrane-associated MtrA from *M. jannaschii* (green) and the cytoplasmic MtrA homologue from *M. fervidus* (orange) were superimposed. Their N-termini are shown as orange and green spheres, and their C-termini as dark-blue and red spheres, respectively. The juxtamembrane segment of MtrA from *M. jannaschii* is drawn in dark-blue, the cobalamin of the MtrA homologue is drawn as a pink stick model.

The soluble domain of membrane-associated MtrA from *M. jannaschii* lacking the transmembrane helix was heterologously expressed in *E. coli* (Supplementary Fig. S5). We were again able to incorporate cobalamin into the apoenzyme by unfolding and refolding the protein, as verified by UV/Vis spectroscopy. Crystallization failed, possibly because the flexible part of the juxtamembrane segment (amino acids 161–220, Supplementary Fig. S5) between the transmembrane helix and the B₁₂ domain disturbed the crystallization process. We therefore partially digested reconstituted MtrA with trypsin to remove this region. Unfortunately, the cobalamin content decreased to less than 50%, which suggested a role of the juxtamembrane segment in stabilizing the prosthetic group. The proteolysis product of MtrA yielded colourless cobalamin-free crystals that diffracted to 1.85 Å resolution (Supplementary Table 1). The structure was solved by molecular replacement using the model of cytoplasmic MtrA homologue as a search template. A malate molecule from the crystallization solution was bound to the binding site of the phosphate group of cobalamin of the MtrA homologue (Supplementary Fig. S6). The overall structures of the two MtrA variants were almost identical (Fig. 3), which was reflected by a root mean square deviation (rmsd) of 0.37 Å for a 127 C_α backbone and a sequence identity of 65%.

Overall architecture of MtrA. The two MtrA variants studied here consist of a single domain with a Rossmann-like open α/β fold (Fig. 4a) that, except for dioldehydratases^{23,24}, ribonucleotide reductases²⁷ and reductive dehalogenases²², is characteristic of B₁₂ enzymes (such as the cobalamin-containing fragment of methionine synthase from *E. coli*, MethH, shown in Fig. 4b). Although they share a common core topology motif $\beta 2\alpha 1\beta 1\alpha 2\beta 3\alpha 3\beta 4\alpha 4$ (Fig. 4), the β -sheet– α -helix arrangements, strand twisting and secondary structure linkers drastically vary between MtrA and other Rossmann-type B₁₂ domains. In fact, MtrA is structurally more related to the functionally distinct pyruvate dehydrogenase (PDB code: 1ik6) or succinyl-CoA synthetase (PDB code: 1euc) domains than to any B₁₂ enzyme (Supplementary Fig. S7). The Z-scores²⁸ of the superimposed structures of MtrA and pyruvate dehydrogenase (PDB code: 1ik6) and succinyl-CoA synthetase (PDB code: 1euc) are 8.4 and 8.1; the Z-scores of MtrA and the most related B₁₂ domains of methionine synthase (1bmt) and methanol cobalamin methyltransferase (2i2x) are 4.5 and 5.5, respectively. The B₁₂-binding protein, which has the highest Z-score (5.6) to MtrA, is monomethylamine corrinoid protein from *M. barkeri* (3ezx).

In MtrA, the core motif is extended by an N-terminally fused segment that is partly associated as an antiparallel β -strand ($\beta 0$) to the central β -sheet and an expanded insertion region between helix $\alpha 3$ and strand $\beta 4$ consisting of a unique meander-like segment and an α -helix ($\alpha 3'$). $\beta 0$ and the unique meander-like segment are involved in cobalamin binding (Fig. 4a). The B₁₂ domains of the corrinoid iron-sulphur proteins also contain an extra N-terminal antiparallel strand, whereas those of methanol cobalamin methyltransferase, methionine synthetase (MethH) and mutases are alternatively extended at the C-terminal end of the shared core by one strand ($\beta 5$) and one helix ($\alpha 5$) (Fig. 4b).

The C-terminal stretch (amino acids 156–170) of truncated MtrA from *M. jannaschii*, which is classified as part of the juxtamembrane segment, turns back from helix $\alpha 4$ towards the C-terminal side of the central β -sheet (Fig. 3). This chain trace does not appear to be due to crystal lattice effects because several salt bridges and hydrophobic contacts between this stretch and the core domain were formed. The remaining 40–50 residues of the juxtamembrane segment appear to be flexible, at least in the truncated form because of the accessibility of this segment for proteolytic cleavage. A flexible connection of the B₁₂ domain to the transmembrane helix is

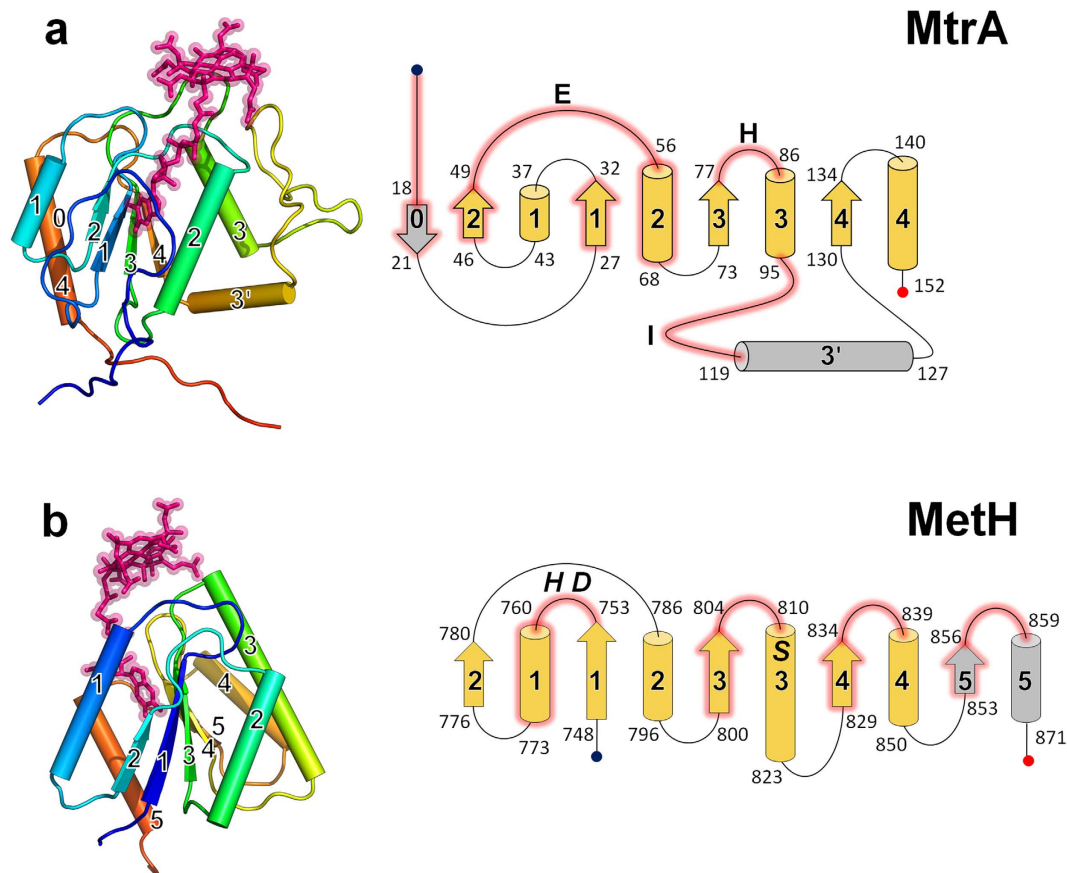


Figure 4. Folds and cobalamin binding of (a) the cytoplasmic MtrA homologue of *M. feravidus* and (b) MetH of *E. coli*. (Left) Three-dimensional secondary structures represented with α -helices as solid tubes, β -sheets as arrows, and loops as strings. The cobalamin-binding pockets in MtrA and MetH are located at opposite side of the central β -sheet. Cobalamin is shown in pink. (Right) Topology diagram with the regions forming the cobalamin binding pocket in pink and the residues of the hydrogen-bonding linkage as single-letter code. Rossmann-type B_{12} domains including MtrA and MetH share the core topology motif $\beta_2\alpha_1\beta_1\alpha_2\beta_3\alpha_3\beta_4\alpha_4$ highlighted in yellow. The secondary structures are named by the numbers of their first and last amino acids.

functionally useful for juggling between the methyl donor and acceptor in analogy to methionine synthetase²⁵, corrinoid iron-sulphur protein methyltransferase¹⁸ and methanol-corrinoid methyltransferase¹⁷, although parts of the juxtamembrane segment might be attached to other subunits of the MtrA–H complex.

The cobalamin binding mode. The cobalamin bound to the cytoplasmic MtrA homologue was positioned at the C-terminal region of the central β -sheet in a base-off/His-on configuration, which confirms previous EPR and mutational analyses¹¹. Cobalamin was bound into a largely preformed binding site inferred from the highly similar structures of the cobalamin-loaded and -unloaded MtrA variants. The corrinoid ring sat exposed on the top of the surface loops following strands β_2 and β_3 and helix α_3 (Fig. 4a), and it was mainly anchored to the polypeptide by the covalent bond between the corrinoid cobalt and His84-ND1 (at a distance of 2.7 Å) protruding from loop β_3 - α_3 . In the obtained crystal form, His35 from another MtrA molecule of the asymmetric unit occupied the sixth ligation site of cobalt, which resulted in a hexacoordinated Co(III) oxidation state (see Fig. 2a). In addition, two propionamide substituents of the corrinoid ring were hydrogen bonded with Asn82-NH or bidentately bonded with the Asn55 amide (the latter was observed only in two molecules of the asymmetric unit) (Supplementary Fig. S8).

The nucleotide tail was accurately embedded into a dominantly hydrophobic pocket lined with β_0 , β_1 , β_2 , helix α_2 , loop β_2 - α_2 and the N-terminal segment (Fig. 4a) and firmly fixed by multiple hydrophobic interactions and specific hydrogen bonds to Asp17-N, Lys52-N, Thr53-OG1 and -N, Gly57-O, and Asn64-ND2. The dimethylbenzimidazole group was sandwiched between the hydrophobic side chains of Tyr18 and Val61. Most residues involved in cobalamin binding were fully conserved in the two MtrA variants (Supplementary Figs S9 and S10).

Superposition studies surprisingly revealed a new binding site for cobalamin in MtrA compared with all other Rossmann-type B_{12} enzymes whose corrinoid rings cluster around the same position (Supplementary Fig. S11). The corrinoid rings are surrounded by different loops and the nucleotide tails bind at different sides of the central β -sheet. Consequently, none of the cobalamin–polypeptide interactions is conserved between MtrA and all other Rossmann-type B_{12} enzymes. Methionine synthase (MetH) is a typical representative of the already established cobalamin binding mode (Figs 4b and 5).

conserved region in MtrA and even allows for the identification of the consensus sequence ¹⁰⁹GAIPF-Y/F-XEN (X: hydrophobic amino acids), which emphasizes its importance. The structural rearrangement could possibly be detected in the structure of a His-unligated Co(I) state, but this structure is not easily obtainable.

Conclusion

Crystal structures of two MtrA variants revealed a detailed view of a novel binding site for cobalamin inside a Rossmann-type domain compared with all other Rossmann-type B₁₂ enzymes studied so far. Nevertheless, several functionally characteristic features were designed in an equivalent manner. They include an exposed corrinoid ring at the top of loops at the C-terminal side of the central β -sheet, an elongated conformation of cobalamin with the nucleotide tail between the β -sheet- α -helix layer, albeit on opposite sides, and a His-Glu-proton donor linkage on the lower axial side of the corrinoid ring.

The structure of cytoplasmic MtrA complexed with cobalamin and the structure of the soluble domain of MtrA without cobalamin were essentially identical. This finding suggested that the MtrA structures observed in this work were relaxed forms. The possible repellent effect of cob(I)alamin towards the histidine residue probably causes a conformational change in the MtrA protein structure (Fig. 1 and Supplementary Fig. S2)^{1,13,29}. From there, the conformational changes could be transmitted further for sodium-ion transport across the cytoplasmic membrane.

Materials and Methods

Bioinformatics searches for the cytoplasmic MtrA homologues. Membrane-associated MtrA from *M. marburgensis* was used as a search query for a general basic local alignment search tool (BLAST) of the NCBI protein database. The discrimination criteria between membrane-associated MtrA and cytoplasmic MtrA homologue were mainly based on the sequence length and the prediction of the membrane segment using the Octopus server³⁰; sequences less than 215 amino acids correspond to cytoplasmic MtrA homologue without the juxtamembrane and transmembrane segments (Supplementary Figs S1 and S5).

Preparation of MtrA proteins. The pET28a expression vector, containing DNA fragments for heterologous expression, was purchased from GenScript (Piscataway, New Jersey, United States); the codon usage of constructs was optimized for expression in *E. coli*. Sequences encoding MtrA were inserted into the expression vector (those of the soluble domain of membrane-associated MtrA from *M. jannaschii* and cytoplasmic MtrA homologue from *M. fervidus* are shown in Supplementary Fig. S5). *E. coli* BL21(DE3) was transformed with the recombinant plasmids. Cells were grown at 37 °C in Luria Bertani (LB) medium supplemented with 50 μ g/ml of kanamycin. When the OD₆₀₀ reached 0.6, 1 mM of isopropyl β -D-thiogalactopyranoside (Roth, Karlsruhe, Germany) was added to induce gene expression. After a 3 h incubation, cells were harvested, washed with 8 mM of phosphate buffer, pH 7.4 supplemented with 150 mM NaCl and 3 mM KCl, and stored at -80 °C for further use.

For expression, we tested gene constructs of the soluble domain of membrane-associated MtrA from the methanogens *M. marburgensis*, *M. evestigatum*, *M. kandleri* and *M. jannaschii*. All genes were highly expressed in *E. coli* BL21(DE3), and a soluble protein was synthesized. The cytoplasmic MtrA homologues from *M. fervidus* and *M. evestigatum* were expressed, but only the protein from *M. fervidus* was obtained in a soluble form in *E. coli* BL21(DE3).

All procedures for purification of MtrA constructs were performed on ice or at 4 °C. Frozen cells containing MtrA were re-suspended in 50 mM of sodium phosphate buffer pH 8.0 containing 0.5 M NaCl, 25 mM imidazole and 5% glycerol (buffer A) and disrupted by sonication (Bandelin Electronic, Berlin, Germany) using a VS70 tip with 50% power, seven times for 2 min with 5 min breaks. The lysate was centrifuged at 30,000 \times g for 45 min at 4 °C. The supernatant was filtered through a 0.45 μ m filter and loaded onto a Ni²⁺-charged HiTrap chelating column (GE Healthcare, Uppsala, Sweden) equilibrated with buffer A. The column was washed extensively with buffer A, and protein was eluted with a linear gradient of imidazole from 25 to 1,000 mM. Fractions were analysed by SDS-PAGE; fractions containing purified MtrA were pooled and concentrated to 1 ml with a 3 kDa cut-off centrifugal filter unit (Millipore).

Cobalamin incorporation. Although methanogenic archaea without cytochromes, including *M. jannaschii* and *M. fervidus*, contain 5-hydroxybenzimidazolyl cobamide (factor III) rather than 5-dimethylbenzimidazolyl cobamide (cobalamin)³¹, cobalamin was used for the reconstitution experiments¹¹. The use of cobalamin instead of factor III, which is commercially unavailable, was possible because the Mtr complex of the cytochrome-free *M. marburgensis*, grown in the presence of dimethylbenzimidazole, was active^{11,31}. All studied MtrA variants were unfolded as follows: 544 μ l of 8.0 M guanidinium hydrochloride pH 7.0, 175 μ l of 0.5 M 3-(*N*-morpholino)propanesulphonic acid (MOPS) pH 7.0 and 17.5 μ l of 1 M dithiothreitol (DTT) were added to 1 ml of a concentrated protein solution. The proteins unfolded at room temperature within at least 2 h. Refolding proceeded in an anoxic tent at room temperature by adding a solution of unfolded protein dropwise into a 25-fold volume of 25 mM Tris-HCl pH 7.6 (44 ml), 150 mM NaCl, 2 mM DTT, 5% glycerol and 0.5 mM methylcobalamin or hydroxocobalamin with gentle stirring to avoid local unspecific aggregation¹¹. In addition, to cleave the His-tag of the cytoplasmic MtrA homologue from *M. fervidus*, thrombin (Sigma-Aldrich, Taufkirchen, Germany) was supplemented to the refolding solution (1.4 mg/ml final concentration). Refolding occurred overnight in an amber glass bottle as cobalamin is light sensitive. All subsequent steps were performed under red light to protect the cobalamin.

We tested the stability of the protein-cobalamin complex by gel filtration. First, the protein refolded with cobalamin was centrifuged under air at 30,000 \times g for 30 min at 4 °C to remove unfolded protein aggregates. The supernatant was filtered through a 0.45 μ m filter and loaded onto a Ni²⁺-charged HiTrap chelating column. The column was extensively washed with 25 mM Tris-HCl pH 7.6 containing 150 mM NaCl, 2 mM DTT and 5% glycerol (GF buffer) to remove unbound cobalamin. Protein was eluted with GF buffer containing 500 mM imidazole and subsequently concentrated in a 3 kDa cut-off centrifugal filter unit. In the case of the cytoplasmic MtrA

homologue from *M. fervidus*, cobalamin and the cleaved His-tag segment were removed by concentration and dilution via ultrafiltration (3-kDa cut-off). The MtrA proteins were then injected onto a HiPrep Sephacryl S100 16/60 (GE Healthcare, Freiburg, Germany) column equilibrated with GF buffer. The amount of cobalamin loaded on the protein sample was estimated from the UV/Vis spectrum (SPECORD S600 Analytik Jena, Jena, Germany). The soluble domains of the membrane-associated MtrA homologues from *M. marburgensis* and *M. kandleri* have less than 40% cobalamin. The soluble domain of membrane-associated MtrA from *M. evestigatum* appeared to contain unspecifically bound cobalamin, as the visible region corresponding to cobalamin had an extremely high absorbance. The only MtrA protein with an approximately 1:1 cobalamin:protein ratio was the soluble domain of the membrane-associated MtrA from *M. jannaschii* and the cytoplasmic MtrA homologue from *M. fervidus*. Therefore, we used these MtrA proteins for crystallization.

Purity of the proteins was controlled by SDS-PAGE. The protein concentration was determined using the Bradford method with the dye reagent and bovine serum albumin from Bio-Rad.

Limited proteolysis by trypsin. Trypsin (Sigma-Aldrich) was added at a trypsin:MtrA ratio of 1:2,000 (w/w) to a solution of refolded cobalamin-bound soluble domain of membrane-associated MtrA from *M. jannaschii* in the presence of 10 mM CaCl₂ (final concentration) and incubated for 6 min at 30 °C. Proteolysis was stopped by adding the irreversible trypsin inhibitor, N_α-tosyl-L-lysine chloromethylketone (0.2 mM; Sigma-Aldrich). The cleaved protein was injected onto a HiPrep Sephacryl S100 16/60 column equilibrated with GF buffer. The eluted protein was analysed by SDS-PAGE.

Protein crystallization. The cytoplasmic MtrA homologue from *M. fervidus*, in complex with either hydroxocobalamin or methylcobalamin, was crystallized using 20 mg/ml protein solution (in GF buffer) under oxic conditions and red light at room temperature. After several months, the hydroxocobalamin complex developed two different crystalline forms, one pink and one orange. Both forms diffracted to a maximum of ca. 6 Å resolution and were therefore not suitable for structural analysis. After approximately one year, only one pink crystal in a new crystalline form appeared in 26% PEG 3000, 100 mM Na citrate pH 5.5. The crystallization drop was prepared by mixing protein and precipitant at a 1:1 ratio using the vapour diffusion method with 1 µl of protein solution (CombiClover Junior Plate, Jena Bioscience, Jena, Germany) and 100 µl of reservoir solution. This crystal diffracted to 3.0 Å. The soluble domain of the membrane-associated MtrA from *M. jannaschii* in the presence of either methylcobalamin or hydroxocobalamin (cleaved by limited proteolysis) was crystallized at 50 mg/ml at 8 °C under oxic conditions and red light. After 2 months of incubation, transparent needle-type crystals were reproducibly obtained in 2.2 M D/L-malate pH 7.6, 100 mM Tris-HCl pH 8.0 under the conditions described above.

Data collection and structural analysis. Crystals of the cytoplasmic MtrA homologue from *M. fervidus* and crystals of the soluble domain of membrane-associated MtrA from *M. jannaschii* were cryoprotected in 25% glycerol and flash-frozen in liquid nitrogen. Diffraction experiments were conducted at 100 K on the beamline X10SA equipped with a PILATUS 6M detector at the Swiss Light Source synchrotron (Villigen). Data were processed with iMOSFLM³². Data of the cleaved soluble domain of the membrane-associated MtrA of *M. jannaschii* were scaled with SCALA, and those of the cytoplasmic MtrA homologue from *M. fervidus* were scaled with AIMLESS in the ccp4 suite³³. The high symmetry space group of the crystal of the cytoplasmic MtrA homologue from *M. fervidus* helped to solve the structure (Supplementary Table 1, I422 space group) using the anomalous signal of cobalt from cobalamin. Single anomalous dispersion (SAD) data were measured at the cobalt K edge. Cobalt atom sites were localized with SHELXC/D³⁴. Phase determination and electron density modification were conducted with the program AutoSol from the PHENIX package³⁵. The model was built using automated AutoBuild from the PHENIX package³⁵. The crystal structure of the soluble domain of the membrane-associated MtrA from *M. jannaschii* was solved by molecular replacement using Molrep from the ccp4 suite³³. The structure of the cytoplasmic MtrA homologue from *M. fervidus* was used as a search model. Both models were then manually improved with COOT³⁶. The model of cytoplasmic MtrA from *M. fervidus* was further refined with REFMAC5³⁷ and that of the soluble domain of membrane-associated MtrA from *M. jannaschii* was refined with PHENIX³⁵. The structure of MtrA homolog from *M. fervidus* contains the cobalamin. Since the crystallographic data for this structure is about 3.0 Å, we impose high geometry restraints to maintain the corrinoid planarity. In a first step, the B₁₂ library was uploaded in Jligand from the ccp4 package and save as a ".cif" file. This file was manually edited to increase the planarity restraint. We use this new library to keep going the refinement using REFMAC5. Non-crystallographic symmetry (NCS) restraints and translation-libration-screw-rotation (TLS)³⁷ were applied to both models. Final models were validated using the MolProbity server (<http://molprobity.biochem.duke.edu>)³⁸. Data quality and refinement statistics are listed in Supplementary Table 1. Figures were generated with PyMOL (Version 1.5, Schrödinger, LLC). The MtrA sequence was aligned with sequences of related proteins from other methanogens using the ClustalW2 server (<http://www.ebi.ac.uk/Tools/msa/clustalw2/>), secondary structures were aligned using ESPript v 3.0 (<http://esprict.ibcp.fr/ESPript/ESPript/>)³⁹ and tertiary structures were superimposed using the CONSURF server (<http://consurf.tau.ac.il/>)⁴⁰ or the Superpose program of the ccp4 suite³³. The folds of MtrA and Meth family proteins (Fig. 4) were compared using the Pro-Origami server (<http://munk.csse.unimelb.edu.au/pro-origami/>)⁴¹.

References

- Gottschalk, G. & Thauer, R. K. The Na⁺-translocating methyltransferase complex from methanogenic archaea. *Biochim. Biophys. Acta* **1505**, 28–36 (2001).
- Thauer, R. K., Kaster, A. K., Seedorf, H., Buckel, W. & Hedderich, R. Methanogenic archaea: ecologically relevant differences in energy conservation. *Nat. Rev. Microbiol.* **6**, 579–591 (2008).
- Kaster, A. K., Moll, J., Parey, K. & Thauer, R. K. Coupling of ferredoxin and heterodisulfide reduction via electron bifurcation in hydrogenotrophic methanogenic archaea. *Proc. Natl. Acad. Sci. USA* **108**, 2981–2986 (2011).

4. Mayer, F. & Müller, V. Adaptations of anaerobic archaea to life under extreme energy limitation. *FEMS Microbiol. Rev.* **38**, 449–472 (2014).
5. Harms, U., Weiss, D. S., Gärtner, P., Linder, D. & Thauer, R. K. The energy conserving N^5 -methyltetrahydromethanopterin:coenzyme-M methyltransferase complex from *Methanobacterium thermoautotrophicum* is composed of 8 different subunits. *Eur. J. Biochem.* **228**, 640–648 (1995).
6. Hippler, B. & Thauer, R. K. The energy conserving methyltetrahydromethanopterin:coenzyme M methyltransferase complex from methanogenic archaea: function of the subunit MtrH. *FEBS Lett.* **449**, 165–168 (1999).
7. Gärtner, P. *et al.* Purification and properties of N^5 -methyltetrahydromethanopterin coenzyme-M methyltransferase from *Methanobacterium thermoautotrophicum*. *Eur. J. Biochem.* **213**, 537–545 (1993).
8. Gärtner, P., Weiss, D. S., Harms, U. & Thauer, R. K. N^5 -methyltetrahydromethanopterin:Coenzyme M methyltransferase from *Methanobacterium thermoautotrophicum* - catalytic mechanism and sodium-ion dependence. *Eur. J. Biochem.* **226**, 465–472 (1994).
9. Harms, U. & Thauer, R. K. Identification of the active site histidine in the corrinoid protein MtrA of the energy-conserving methyltransferase complex from *Methanobacterium thermoautotrophicum*. *Eur. J. Biochem.* **250**, 783–788 (1997).
10. Sauer, K. & Thauer, R. K. His⁸⁴ rather than His³⁵ is the active site histidine in the corrinoid protein MtrA of the energy conserving methyltransferase complex from *Methanobacterium thermoautotrophicum*. *FEBS Lett.* **436**, 401–402 (1998).
11. Harms, U. & Thauer, R. K. The corrinoid-containing 23-kDa subunit MtrA of the energy-conserving N^5 -methyltetrahydromethanopterin:coenzyme M methyltransferase complex from *Methanobacterium thermoautotrophicum*. EPR spectroscopic evidence for a histidine residue as a cobalt ligand of the cobamide. *Eur. J. Biochem.* **241**, 149–154 (1996).
12. Weiss, D. S., Gärtner, P. & Thauer, R. K. The energetics and sodium-ion dependence of N^5 -methyltetrahydromethanopterin:coenzyme-M methyltransferase studied with cob(I)alamin as methyl acceptor and methylcob(III)alamin as methyl donor. *Eur. J. Biochem.* **226**, 799–809 (1994).
13. Kräutler, B. In *Vitamin B₁₂ and B₁₂ proteins* (eds B. Kräutler, D. Arigoni, & B. Golding) 4–43 (Wiley-VCH, 1998).
14. Banerjee, R. & Ragsdale, S. W. The many faces of vitamin B12: catalysis by cobalamin-dependent enzymes. *Annu. Rev. Biochem.* **72**, 209–247 (2003).
15. Sukumar, N. Crystallographic studies on B12 binding proteins in eukaryotes and prokaryotes. *Biochimie* **95**, 976–988 (2013).
16. Drennan, C. L., Huang, S., Drummond, J. T., Matthews, R. G. & Ludwig, M. L. How a protein binds B₁₂-a 3.0-Å X-ray structure of B₁₂-binding domains of methionine synthase. *Science* **266**, 1669–1674 (1994).
17. Hagemeyer, C. H., Krüer, M., Thauer, R. K., Warkentin, E. & Ermler, U. Insight into the mechanism of biological methanol activation based on the crystal structure of the methanol-cobalamin methyltransferase complex. *Proc. Natl. Acad. Sci. USA* **103**, 18917–18922 (2006).
18. Kung, Y. *et al.* Visualizing molecular juggling within a B₁₂-dependent methyltransferase complex. *Nature* **484**, 265–269 (2012).
19. Svetlitchnaia, T., Svetlitchnyi, V., Meyer, O. & Dobbek, H. Structural insights into methyltransfer reactions of a corrinoid iron-sulfur protein involved in acetyl-CoA synthesis. *Proc. Natl. Acad. Sci. USA* **103**, 14331–14336 (2006).
20. Mancía, F. *et al.* How coenzyme B₁₂ radicals are generated: The crystal structure of methylmalonyl-coenzyme A mutase at 2 Å resolution. *Structure* **4**, 339–350 (1996).
21. Reitzer, R. *et al.* Glutamate mutase from *Clostridium cochlearium*: the structure of a coenzyme B12-dependent enzyme provides new mechanistic insights. *Structure* **7**, 891–902 (1999).
22. Bommer, M. *et al.* Structural basis for organohalide respiration. *Science* **346**, 455–458 (2014).
23. Yamanishi, M. *et al.* The crystal structure of coenzyme B12-dependent glycerol dehydratase in complex with cobalamin and propane-1,2-diol. *Eur. J. Biochem.* **269**, 4484–4494 (2002).
24. Shibata, N. *et al.* A new mode of B12 binding and the direct participation of a potassium ion in enzyme catalysis: X-ray structure of diol dehydratase. *Structure* **7**, 997–1008 (1999).
25. Ludwig, M. L. & Matthews, R. G. Structure-based perspectives on B₁₂-dependent enzymes. *Annu. Rev. Biochem.* **66**, 269–313 (1997).
26. Kim, J., Gherasim, C. & Banerjee, R. Decyanation of vitamin B₁₂ by a trafficking chaperone. *Proc. Natl. Acad. Sci. USA* **105**, 14551–14554 (2008).
27. Sintchak, M. D., Arjara, G., Kellogg, B. A., Stubbe, J. & Drennan, C. L. The crystal structure of class II ribonucleotide reductase reveals how an allosterically regulated monomer mimics a dimer. *Nat. Struct. Biol.* **9**, 293–300 (2002).
28. Holm, L. & Rosenström, P. Dali server: conservation mapping in 3D. *Nucl Acids Res* **38**, W545–W549 (2010).
29. Hayashi, T. *et al.* Co(II)/Co(I) reduction-induced axial histidine-flipping in myoglobin reconstituted with a cobalt tetrahydrocorrin as a methionine synthase model. *Chem. Commun.* **50**, 12560–12563 (2014).
30. Viklund, H. & Elofsson, A. OCTOPUS: improving topology prediction by two-track ANN-based preference scores and an extended topological grammar. *Bioinformatics* **24**, 1662–1668 (2008).
31. Stupperich, E., Steiner, I. & Eisinger, H. J. Substitution of Co alpha-(5-hydroxybenzimidazolyl)cobamide (factor III) by vitamin B12 in *Methanobacterium thermoautotrophicum*. *J. Bacteriol.* **169**, 3076–3081 (1987).
32. Battye, T. G. G., Kontogiannis, L., Johnson, O., Powell, H. R. & Leslie, A. G. W. iMOSFLM: a new graphical interface for diffraction-image processing with MOSFLM. *Acta Crystallogr. D* **67**, 271–281 (2011).
33. Winn, M. D. *et al.* Overview of the CCP4 suite and current developments. *Acta Crystallogr. D* **67**, 235–242 (2011).
34. Sheldrick, G. M. A short history of SHELX. *Acta Crystallogr. A* **64**, 112–122 (2008).
35. Afonine, P. V. *et al.* phenix.model_vs_data: a high-level tool for the calculation of crystallographic model and data statistics. *J. Appl. Crystallogr.* **43**, 669–676 (2010).
36. Emsley, P. & Cowtan, K. Coot: model-building tools for molecular graphics. *Acta Crystallogr. D* **60**, 2126–2132 (2004).
37. Murshudov, G. N., Vagin, A. A. & Dodson, E. J. Refinement of macromolecular structures by the maximum-likelihood method. *Acta Crystallogr. D* **53**, 240–255 (1997).
38. Chen, V. B. *et al.* MolProbity: all-atom structure validation for macromolecular crystallography. *Acta Crystallogr. D* **66**, 12–21 (2010).
39. Gouet, P., Robert, X. & Courcelle, E. ESPript/ENDscript: extracting and rendering sequence and 3D information from atomic structures of proteins. *Nucleic Acids Res.* **31**, 3320–3323 (2003).
40. Celniker, G. *et al.* ConSurf: using evolutionary data to raise testable hypotheses about protein function. *Isr. J. Chem.* **53**, 199–206 (2013).
41. Stivala, A., Wybrow, M., Wirth, A., Whisstock, J. C. & Stuckey, P. J. Automatic generation of protein structure cartoons with Pro-origami. *Bioinformatics* **27**, 3315–3316 (2011).

Acknowledgements

We thank Prof. Dr. Rolf Thauer for discussions and helpful suggestions, Prof. Dr. Hartmut Michel for continuous support, and the staff of the PXII beamline at Swiss Light Source (Villigen, Switzerland) and the staff of the PXI beamline at SOLEIL Synchrotron (Saclay, France) for their help during data collection and X-ray crystallographic structural analyses. We also thank Jürgen Koch for laboratory maintenance. This work was supported by a grant of the Max Planck Society to Rolf Thauer and a grant of the PRESTO program from the Japan Science and Technology Agency to S.S.

Author Contributions

S.S. directed the research. S.S. and T.W. designed the study. T.W. prepared, crystallized and characterized proteins. U.E. and T.W. collected synchrotron data. T.W. performed X-ray crystallographic analyses. S.S., T.W. and U.E. interpreted the data and wrote the manuscript.

Additional Information

Supplementary information accompanies this paper at <http://www.nature.com/srep>

Competing financial interests: The authors declare no competing financial interests.

How to cite this article: Wagner, T. *et al.* MtrA of the sodium ion pumping methyltransferase binds cobalamin in a unique mode. *Sci. Rep.* **6**, 28226; doi: 10.1038/srep28226 (2016).



This work is licensed under a Creative Commons Attribution 4.0 International License. The images or other third party material in this article are included in the article's Creative Commons license, unless indicated otherwise in the credit line; if the material is not included under the Creative Commons license, users will need to obtain permission from the license holder to reproduce the material. To view a copy of this license, visit <http://creativecommons.org/licenses/by/4.0/>